Inactivation mechanisms of *Escherichia coli* O157:H7 and *Salmonella enterica* by free residual chlorine

Journal:	*Environmental Science: Water Research & Technology*
Manuscript ID	EW-ART-05-2022-000382.R1
Article Type:	Paper

Water Impact Statement

Free residual chlorine level serves as a proxy for disinfection efficacy and chemical safety in a variety of applications including drinking water and swimming water treatment and distribution systems. Thus, elucidating the mechanisms of pathogen inactivation at such levels is of significant interest, with broad applications in fine-tuning dosing strategies for fresh produce wash and meat processing plants.

Inactivation mechanisms of *Escherichia coli* O157:H7 and *Salmonella enterica* by free residual chlorine

Mohammadreza Dehghan Abnavi[a], Taban Larimian[b], Parthasarathy Srinivasan[c], Daniel Munther[c], Chandrasekhar R. Kothapalli[a, *]

[a] Department of Chemical and Biomedical Engineering, 2121 Euclid Avenue, Cleveland State University, Cleveland, OH 44115, USA

[b] Department of Mechanical Engineering, 2121 Euclid Avenue, Cleveland State University, Cleveland, OH 44115, USA

[c] Department of Mathematics, 2121 Euclid Avenue, Cleveland State University, Cleveland, OH 44115, USA

*Corresponding author

Chandrasekhar Kothapalli, PhD, Professor, Fenn Hall 455, Chemical and Biomedical Engineering, Cleveland State University, Cleveland, OH 44115, USA.

Email: c.kothapalli@csuohio.edu; Tel: 1-216-687-2562.

Abstract

The sub-cellular mechanisms by which residual free chlorine (FC) inactivates *E. coli* O157:H7 and *S. enterica* in the absence of organic matter was investigated. The average removal rates for *E. coli* were 38% – 99% after a 1 min exposure to 0.12–0.5 mg·L^{-1} FC, while that of *S. enterica* were 10% – 50% after exposure to 0.5–2.0 mg·L^{-1} FC. Chlorination caused significant membrane

structural damage and reduced membrane potential. Low FC levels or short exposure times had a modest impact on *S. enterica*. Cell metabolic activity decreased over time for all initial FC levels, and with increasing FC levels at each time point. Total ATP levels increased in the first minute post-chlorination, while the intracellular ATP levels decreased with increasing FC levels and exposure time, likely due to ATP leakage. The depolarized *E. coli* density reached a plateau after the first 2 min at FC ≥ 0.5 mg·L^{-1} while that of *S. enterica* took 5 min to reach a plateau even at FC ≥ 1 mg·L^{-1}, indicating their ability to withstand chlorination. Residual FC levels are sufficient to induce damage to cellular organelles and compromise their survival, and the mechanism of injury depends on FC levels and exposure time.

Key Words: *E. coli*, *S. enterica*, inactivation mechanisms, metabolic activity, membrane potential, ATP levels.

1 Introduction

　　Chlorine is one of the most widely used sanitizers for microbial control in processes such as drinking water and wastewater treatments owing to its strong oxidizing capacity, easy accessibility and low cost.[1, 2] It is also used as a disinfectant in the food industry to sanitize fresh produce and fruits, mitigating pathogen cross-contamination.[3] Numerous studies have explored the optimal free chlorine (FC) concentration and contact time on the disinfection processes in the agri-food industry, to maximize chlorine efficacy[4-7], reduce cross-contamination risk[8], minimize the formation of chlorine by-products[9-11], keep the texture of fresh produce intact, and eliminate off-taste and smell[8]. Almost all of these studies measuring pathogen viability post-exposure to chlorine rely on traditional culture-based methods such as colony forming units (CFU)[12] or the most probable number (MPN) assay[13]. However, the disinfection performance cannot always be reliably

obtained from culture-based methods such as plate-counting[14, 15]. For instance, when low concentrations of chlorine were used, some surviving bacteria could potentially lose their ability to proliferate and/or migrate, yet could still contribute to disease outbreaks[16-18]. Moreover, under favorable conditions, the surviving pathogens could self-repair their damage (after chlorine exposure) over time and recover their ability to proliferate and/or migrate[18, 19]. Thus, despite their relative ease of use and low cost, traditional culture-based methods could overestimate the disinfectant sanitization efficacy and underestimate pathogen tolerance to sanitizers.[14]

Since the conventional plate-count methods are sub-optimal for evaluating disinfection efficiency, there is a need for alternative methods to assess the time-dependent effect of chlorine on pathogens and elucidate the underlying mechanisms of action. Various techniques that were developed to study eucaryote response to environmental changes, such as assessing the changes in membrane integrity, metabolic activity, membrane potential, and damage to deoxyribonucleic acid (DNA) and messenger ribonucleic acid (mRNA), to name a few, are being extended to procaryotes. [16, 20] One such tool to quantitatively analyze the changes in cellular organelles or function, and thereby the response to a disinfection process, is flow cytometry.[17] Most sanitizers have been shown to damage the bacterial cell wall[16, 18, 20] and flow cytometry is useful to quantify the effects of chemical disinfectants on the integrity of the cellular membrane.[21] Using various fluorescent dyes, flow cytometry can assess the total and intact cell count. Similarly, fluorescent stain combinations such as calcein AM/propidium iodide (PI) and SYBR Green/SYTO enables one to determine the cellular membrane integrity during the disinfection process.[22] Another method to measure cell viability is to quantify the change in adenosine triphosphate (ATP) molecule concentration, which stands as an indicator of the cell's metabolic activity. Monitoring the ATP concentration can show how the microorganisms respond to the sanitizer and thereby can help to

quantify the number of active cells. However, ATP detection is not reliable when the total number of cells are lower than ten thousand.[23] Flow cytometry analysis and ATP measurement are also rapid and accurate methods that have the potential for automation or high-throughput analyses.[22]

The antimicrobial effect(s) of a few disinfectants has been reported, including the effect of ozone[22], chlorine dioxide[24, 25], isopropyl alcohol[26], slightly acidic electrolyzed water[27], and free chlorine.[16-18] Chemical agents interfere with cellular membrane and alter the cell permeability and/ or membrane potential.[26] Bacterial exposure to chlorine caused extensive permeabilization of the cytoplasmic membrane, but there was no detectable relation between the occurrence of membrane permeabilization and cell death.[18] Chlorine treatment reduced the intact viable cell count, while prolonged exposure caused both a reduction in the total cell count and fluorescence intensity, likely indicating a breakdown of the cell membrane.[17] Low doses of chlorine (< 5 mg·L^{-1}) can affect membrane permeability and consequently increase the extracellular ATP levels, indicating the leakage of intracellular ATP.[16] During the processing of fresh-cut produce, although the initial total chlorine levels could be as high as 200 ppm (US FDA), the target range for disinfection effects of FC is much lower (< 10 mg·L^{-1}).[28] On the other hand, municipal water systems target residual chlorine levels of around $0.25 - 2$ mg·L^{-1} in potable water.[29] Thus, it is beneficial to identify the antimicrobial effects of FC at these residual doses (≤ 2 mg·L^{-1}) and elucidate the mechanisms by which FC affects bacteria at those levels.

The objectives of this study were to (i) investigate the disinfection efficacy and the inactivation dynamics of FC (≤ 2 mg·L^{-1}) on *E. coli* and *S. enterica*, and (ii) identify the mechanisms by which FC inactivates *E. coli* and *S. enterica* at those levels using quantitative and qualitative techniques. These two bacterium types have been linked to numerous outbreaks in a variety of settings (e.g., drinking water hygiene, wastewater sanitation, agri-food industry, medical and healthcare

network) and therefore widely explored for disinfection and sterilization efficacy studies.[30] Immunolabeling was used to quantitatively detect time-dependent and FC-concentration dependent changes in membrane potential, ATP and cell survival. Conventional MPN cell count was used to quantify the cell density in these latter cultures for comparison purposes. Furthermore, scanning electron microscopy (SEM) and fluorescence microscopy were used to qualitatively observe the morphological changes in *E. coli* and *S. enterica* during the FC inactivation process. Finally, the advantages and limitations of these techniques for assessing and monitoring disinfection efficiency during chlorination of these bacteria were discussed.

2 Methods

2.1 Bacterial strains and preparation of suspension

Non-pathogenic *E. coli* O157:H7 (ATCC # 1428) and *S. enterica* subsp. (ATCC # 53647) strains were used in this study. These strains responded to antimicrobial interventions in a manner similar to their pathogenic counterparts (e.g., *E.coli* O157:H7) and were recommended by the USDA for scientific research.[31, 32] After opening lyophilized vials, one loop of frozen cells was transferred into tryptic soy agar/broth (TSB, ATCC Medium 18) for *E. coli* culture or into nutrient agar/broth (ATCC Medium 3) for *S. enterica* culture and placed in a shaking incubator (120 rpm) overnight (37 °C). The respective incubated broths were further sub-cultured with nalidixic acid until the final broth had a concentration of 50 mg·L^{-1} nalidixic acid. After incubation, cells were harvested by centrifuging at $3000 \times g$ for 10 min, and the collected cells were washed twice with sterile $1\times$ phosphate buffered saline (PBS) and subsequently resuspended in 50 mL of PBS. Individual strains were constituted at a concentration of approximately 9-log MPN·mL^{-1} and were

used to prepare 6-log MPN·mL^{-1} solutions for disinfection experiments. All the chemicals and media were purchased from Sigma-Aldrich unless stated otherwise.

2.2 Chlorine disinfection experiments

These experiments were designed to determine the mechanisms by which chlorine inactivates *E. coli* and *S. enterica* in the absence of an organic load. All disinfection experiments were done in 500 mL flasks containing 250 mL of tap water. The pH was regulated to 6.5 by adding 0.1 M citrate buffer. After sterilizing flasks for 20 min at 121 °C, an appropriate density of cells from the suspensions were transferred to the flasks to yield a final bacterial concentration of 6-log MPN·mL^{-1}, and the flasks were refrigerated (4 °C). Then 0.7, 1.4, 2.8, 5.6, or 11.2 mL of 1000-fold diluted 4.5% sodium hypochlorite (BCS Chemicals, Redwood City, CA, USA) was added to the respective flasks to achieve 0.125, 0.25, 0.50, 1.0, or 2.0 mg·L^{-1} initial free chlorine (FC) concentration solutions. Flasks were continuously mixed (200 rpm) using an overhead stirring apparatus equipped with sterile paddles. Samples were taken from the reaction vessels at the desired contact times and added to tubes containing sterile deionized water with 0.1% (wt./vol.) sodium thiosulfate to immediately neutralize residual chlorine. Chlorine concentrations were determined immediately after taking the sample, using the N, N-diethyl-p-phenylenediamine (DPD) method, with a Chlorine Photometer (CP-15, HF Scientific Inc., Ft. Myers, FL). Bacteria survival was measured by counting cells (overnight incubation at 37 °C) via a modified Most-Probable-Number (MPN) method using 48-well deep microplates.[33] All experiments were independently replicated three times.

2.3 Disinfection mechanisms of free chlorine

Experiments were carried out to investigate the bactericidal mechanisms of free chlorine in terms of the effect on the culturability, morphology of the cells, metabolism, and the permeability of the outer cell membrane.

2.3.1 Scanning electron microscopy (SEM) analysis

The changes in bacteria morphology were assessed using SEM. Bacteria suspensions before and after adding free chlorine (at specific time points) were first centrifuged at $2000 \times g$ for 5 min, supernatant discarded, and incubated with 2% glutaraldehyde solution overnight at 4 °C. The cell suspensions were washed with ethanol gradient (70% – 100%) solutions to remove excessive glutaraldehyde, incubated with 1 mL of isoamyl acetate for one hour, and air-dried for two days under vacuum in a desiccator. Samples were gold sputtered (SPI sputter model 13131; 350 Å, 40 mA, 10 Torr, 10 sec) and imaged using a Inspect F50 field-emission SEM (FEI Company, Hillsboro, OR) to assess the changes in cell morphology and visible damages to cells. The images were analyzed using NIH ImageJ to determine changes in bacterial morphology.

2.3.2 Live/Dead analysis using fluorescence imaging

A LIVE/DEAD BacLight™ bacterial viability kit (Thermofisher, L7007) composed of two separate fluorescent dyes (SYTO 9 and Propidium iodide (PI)) was used to test the viability of chlorine-exposed cells. SYTO 9 is a green-fluorescent nucleic acid stain and stains all cells, while PI is a red-fluorescent nucleic acid stain that can only penetrate damaged membranes. The Live/Dead assay was performed immediately after collection of the samples as per the manufacturer's instructions, Briefly, 3 µL of the stained mixtures was added to 1 mL of the bacterial samples from the disinfection experiments and mixed thoroughly and incubated in the dark at room temperature for 30 min. Then, the fluorescence images were obtained using a Zeiss AxioVert A1 inverted fluorescence microscope under both phase contrast and fluorescent

channels, using Axiocam C1 digital camera and Axiovision data acquisition software. At least five images were taken per condition in each well (n = 3 wells/condition) at random locations.

2.3.3 Live/Dead analysis using fluorescence spectroscopy

The LIVE/DEAD BacLight™ bacterial viability kit described above was used to measure the ratio of live to dead cells. The dead cell stock solution was made by exposing cells to 0.25 mg·L^{-1} FC for 15 min. Suspensions of various ratios of live/dead cells (**Table 1**) were used to obtain the standard curve (**Suppl. Fig. 1**) which helped in determining the live/dead cell ratio in samples from disinfection experiments. The assay was done as per manufacturer's instructions: 100 µL of disinfection samples and the standard live/dead suspension were added to a 96 well-plate, and 100 µL of the 10× diluted stained mixture was added to each well. Stained samples were incubated at room temperature in the dark for 15 min. Fluorescence measurement was obtained using an F-7000 Fluorescence Spectrophotometer (Hitachi) by setting the excitation wavelength at 485 nm and emission wavelengths at 530 nm (FI_{Green}) or 630 nm (FI_{Red}). The live/dead cell ratio is defined as $Ratio_{G/R} = FI_{Green}/FI_{Red}$. To obtain the standard curve, the $Ratio_{G/R}$ vs. standard live/dead percentage was plotted (Suppl. Fig. 1) and the live/dead cell percentage of disinfection samples were measured using this standard curve.

Table 1 Volumes of live and dead cell suspensions mixed to achieve various proportions of live/dead cells for fluorescence microplate readers.

Ratio of Live Cells (%)	Live Cell Suspension (mL)	Dead Cell Suspension (mL)
0	0.0	1.0
10	0.1	0.9
25	0.25	0.75
50	0.5	0.5
75	0.75	0.25
90	0.9	0.1
100	1.0	0.0

8

2.3.4 Total adenosine triphosphate (ATP) levels

Total ATP concentration was measured using an ATP determination kit (Thermofisher, A22066) and a luminometer (SynergyTM 4, BioTek, USA). The standard reaction solution was prepared based on the kit protocols by mixing different reagents of the kit. Then some standard ATP solutions with different concentrations were prepared to obtain the standard curve (Fig. 2). After that, 90 µL of the standard reaction solution (provided with the assay kit) was added to the wells of a 96-well plate and the background luminescence was measured. Then 10 µL of each standard solution and samples from disinfection experiments were added to the wells and luminescence was read again. After subtracting the background luminescence noise, first the standard curve was generated (**Suppl. Fig. 2**), followed by the measurement of ATP concentration of disinfection samples.

2.3.5 MTT assay for cellular metabolic activity

One method for measuring metabolic activity is to incubate cells with water-soluble tetrazolium salt (WST-1), which is cleaved into a colored formazan product by metabolically active cells. The effect of chlorine on cell metabolic activity and thus proliferation was assessed through a CytoSelect™ MTT Cell Proliferation Assay (Cell Biolabs, Inc., San Diego, CA, USA) as described elsewhere.[27] Aliquots (1 mL) taken from disinfection experiments at various treatment time points (0 – 10 min) were added to 9 mL of 0.01 M PBS solutions with 0.1% (wt./vol.) sodium thiosulfate to quench the residual chlorine. After 5 min of neutralization, samples were centrifuged at 5000 rpm for 5 min. The supernatant was discarded, and cells resuspended in 1 mL of sterile tryptic soy broth. A 100 µL aliquot of this bacteria suspension was added to 96-well culture plates, 10 µL of MTT reagent added to each well, and incubated at 37 °C for 4 h in the dark. To this, 100

µL of detergent solution (provided in the kit) was added to each well and incubated in dark for another 2 h. The final mixture was vibrated in an incubator shaker for 10 min to dissolve the precipitate. and the absorbance of each well measured at an OD of 540 nm with a microplate reader (SynergyH1, BioTek, Vermont, USA). Inhibition rate of bacteria proliferation was reported as OD values.

2.3.6 Bacteria membrane potential

A BacLight™ Bacterial Membrane Potential Kit (Thermofisher, B34950) was used to determine the cellular membrane potential during the disinfection process. This kit contains two stains: carbocyanine dye DiOC2(3) (3,3-diethyloxacarbocyanine iodide, Component A) and CCCP (carbonyl cyanide 3-chlorophenylhydrazone, Component B), both in DMSO. DiOC2(3) exhibits green fluorescence in all bacterial cells, but the fluorescence shifts toward red emission as the dye molecules self-associate at the higher cytosolic concentrations caused by larger membrane potentials. Proton ionophores such as CCCP destroy membrane potential by eliminating the proton gradient. Briefly, 1 mL of the chlorine-treated bacteria, collected at various time points, was added to 9 mL of sterilized 0.01 M PBS solution containing 0.1% (wt./vol.) sodium thiosulfate and centrifuged at $2000 \times g$ for 5 min. Then the supernatant was removed, and cells were resuspended in 1 mL sterile 0.01 M PBS solution. One milliliter aliquots of bacteria suspensions (n = 3) for each time point were added to Falcon Round-Bottom polypropylene flow cytometry test tubes (Fisher Scientific). Flow cytometry (FCM) analysis needed three processed samples: stained, depolarized control, and an unstained control. One of the tubes is unstained control and no stains will be added to it. To make the depolarized control, 10 µL of 500 µM CCCP (Component B) and 10 µL of 3 mM DiOC2(3) (Component A) were added to another tube and mixed. In the last tube, only 10 µL of 3 mM DiOC2(3) (Component A) was added and mixed, and samples

incubated at room temperature for 15–30 min. The stained bacteria were assayed in a flow cytometer (BD LSRFortessa™ X-20 Flow Cytometer, Amersham Biosciences Corp., NJ, USA) equipped with a laser emitting at 488 nm. Green fluorescence was collected in the FL1 channel (520 nm) whereas red fluorescence was collected in the FL3 channel (613 nm).

2.4 Statistical analysis

All experiments were carried out in triplicates. Data was represented as arithmetic average ± standard deviation (SD) unless specific otherwise. MINITAB Statistical Software package (Version 17) was used to perform one-way analysis of variance (ANOVA) and Tukey's test. A p-value < 0.05 between groups was considered statistically significant.

3 Results and discussion

3.1 Inactivation efficiency of chlorine and disinfection kinetics model

The change in FC concentration as well as the inactivation of *E. coli* and *S. enterica* under those FC concentrations was assessed over 10 min at 4 °C. A rapid decay in FC concentration within the first minute of chlorine addition, followed by a slow decay was noted (**Fig. 1**), most possibly due to reaction of chlorine with various organic compounds in the bacterial cell wall. Compounds that include nitrogen in their molecular structure react quickly with chlorine, while other organic compounds have smaller reaction rates with chlorine.[34] Also, the change in the FC concentration for experiments with FC of 0.25 and 0.5 mg·L⁻¹ were almost the same, which shows that the chlorine demand is related to the bacterial load and not the initial chlorine concentration.

11
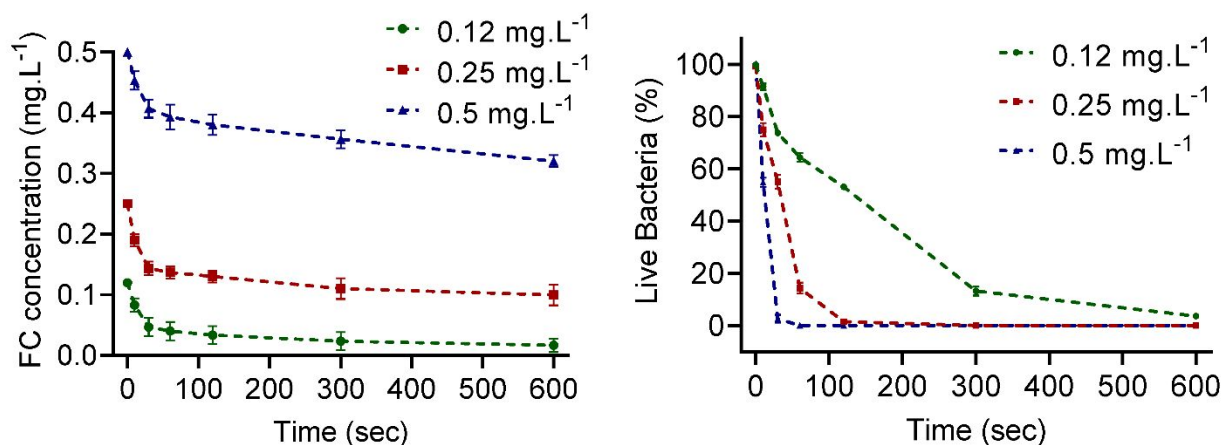
A. *E. coli*

B. *S. enterica*
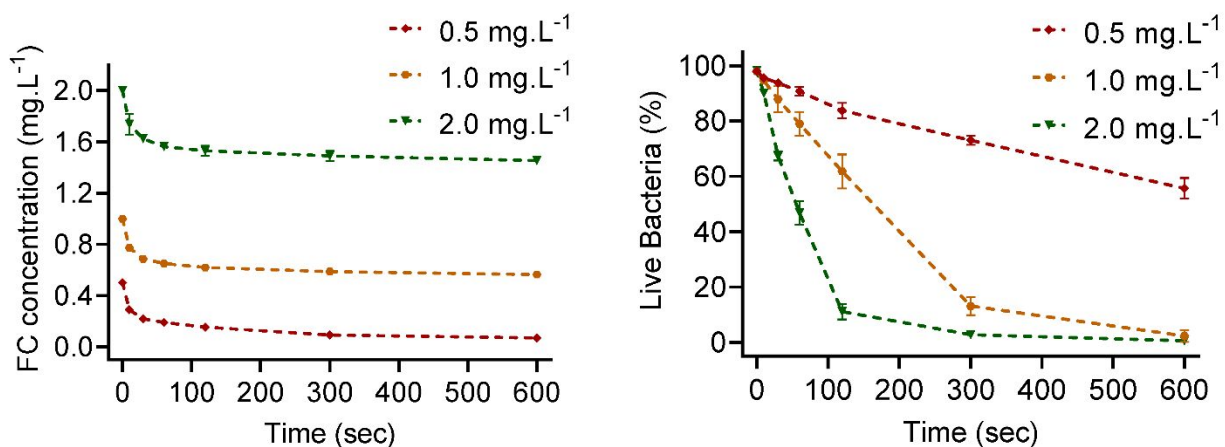
Fig. 1 Free chlorine decay and survival rates (culture-based MPN method) of *E. coli* (A) and *S. enterica* (B). *E. coli* were exposed to 0.12, 0.25 and 0.50 mg·L⁻¹ initial free chlorine (FC) concentrations, while *S. enterica* were exposed to 0.5, 1.0 and 2.0 mg·L⁻¹ FC concentrations. Reaction conditions: pH = 7.1, T = 4 °C, initial concentration of bacteria: ~ 10⁶ MPN·mL⁻¹.

From the culture-based MPN method, the average removal rates of *E. coli* were 38%, 87%, and 99%, respectively, after exposure to 0.12, 0.25, and 0.5 mg·L⁻¹ FC for 1 min (Fig. 1A). For all three FC concentrations tested, no surviving *E. coli* could be measured after 10 min. These results support our hypothesis that chlorination has a significant effect on *E. coli* inactivation, and in agreement with our previous results.[33] Previously, we have calculated that the average inactivation

coefficient (α_{Max}) of *E. coli* by FC was 70.4 ± 3.2 L·mg^{-1}·min^{-1} (3.69 µM·min^{-1}) and the CT values

for 2- to 4-log inactivation of *E. coli* were in the range of 0.065 to 0.131 mg·min·L^{-1}. Increasing

the chlorine concentration lowered the time for removal of 99% bacterial load from 10 min for FC

of 0.12 mg·L^{-1} to 2 min for FC of 0.25 mg·L^{-1} and 30 seconds for FC of 0.5 mg·L^{-1} (Fig. 1A).

The average removal rates of *S. enterica* were 10%, 23%, and 50%, respectively, after exposure

to 0.5, 1.0, and 2.0 mg·L^{-1} FC for 1 min (Fig. 1B). After a 10-min exposure, no surviving *S. enterica*

could be measured for FC ≥ 1 mg·L^{-1}, although 50% of the *S. enterica* cells survived at 0.5 mg·L^{-1} FC. It appears that chlorination has a modest impact on *S. enterica* at low FC concentrations or

at low exposure times (< 2 min). We calculated that the average inactivation coefficient (α_{Max}) of

S. enterica by FC is 4.56 ± 0.12 L·mg^{-1}·min^{-1} (0.24 µM·min^{-1}) and the CT values for a 2- to 4-log

inactivation of *S. enterica* are in 1.01 – 2.021 mg·min·L^{-1} range.

## 3.2 Morphometric analysis using SEM

The structural changes in *E. coli* and *S. enterica* due to chlorination were observed using SEM.

The untreated *E. coli* cells exhibited a smooth, intact surface with a rod-shaped morphology having

an average length of 1.25 µm and average width of 0.4 µm (**Fig. 2**). Visible damage to the cell

surface could be noted even with a 10-sec exposure to 0.5 mg·L^{-1} FC, 30 sec exposure to 0.25

mg·L^{-1} FC and 60 sec exposure to 0.12 mg·L^{-1} FC, with the cell surface appearing rough and

wrinkled. With increasing time, holes and fibrous structures were evident on the cell surface,

indicating a compromise in the cell integrity and possible release of intracellular components.

Higher FC levels and prolonged exposure destroyed the cell wall and disintegrated the cell,

reducing it to a pulp-like appearance.

A similar pattern was noted in the SEM images taken for S. enterica exposed to FC for 10 min (**Fig. 3**). In the control cultures, *S. enterica* were rod-shaped with a relatively smaller aspect ratio (average length of 0.9 μm, average width of 0.5 μm) as compared to *E. coli*. Significant rounding of cells and damage to cell surface was evident starting at 120 sec exposure to 2.0 mg·L^{-1} FC and 300 sec exposure to 1.0 mg·L^{-1} FC. However, most cells appeared intact at 0.5 mg·L^{-1} FC exposure, even at 10 min. These SEM observations correlate to and complement the quantitative survival data for *E. coli* (Fig. 1A) and *S. enterica* (Fig. 1B), confirming that chlorination causes significant cell membrane damage in *E. coli*. Previous studies reported that *E. coli* and *S. enterica* did not survive at FC ≥ 3.66 mg·L^{-1} independent of the initial FC levels,[35] while *S. enterica* exposed to 3 mg·L^{-1} FC for 2 min became viable-but-nonculturable (VBNC) with higher FC levels leading to complete cell destruction.[36] Our study here shows that even lower FC levels with prolonged exposure are sufficient to inactivate these pathogens in the absence of an organic load.

Irreversible damage in the surface structure is a major step for microbial inactivation during chlorination. The N-terminal amino acids of peptidoglycan located on the *E. coli* wall could be oxidized during chlorination leading to significant damage to the cell surface, resulting in the release of vital intracellular compounds.[37] However, the lethal effects of FC on gram-negative cells such as *E. coli*, observed most prominently as cell membrane damage, could be countered by the addition of minute quantities of organic matter.[18] Similar morphological changes in *E. coli* and *Salmonella* were noted when exposed to sub-inhibitory chlorine concentrations, *i.e.*, roughness, deformation, holes, wrinkles, clustering, shrinkage, membrane breakdown, and structural collapse, possibly due to elevated levels of oxidative stress and intracellular reactive oxygen species.[38, 39]
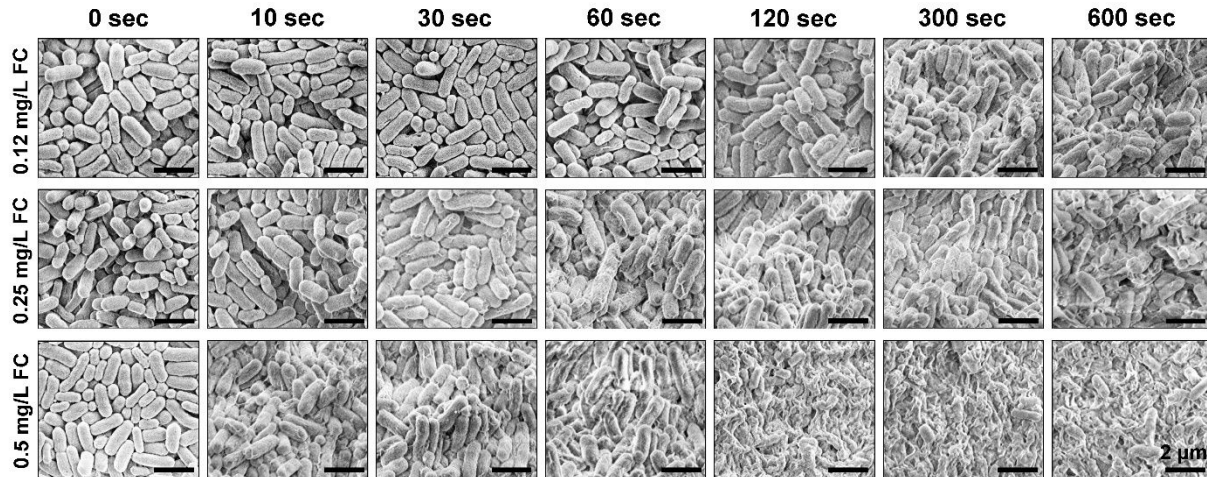
Fig. 2 Representative SEM images of *E. coli* treated with various initial FC doses. Images corresponding to 0 sec refer to the control sample, *i.e.*, prior to chlorine addition.
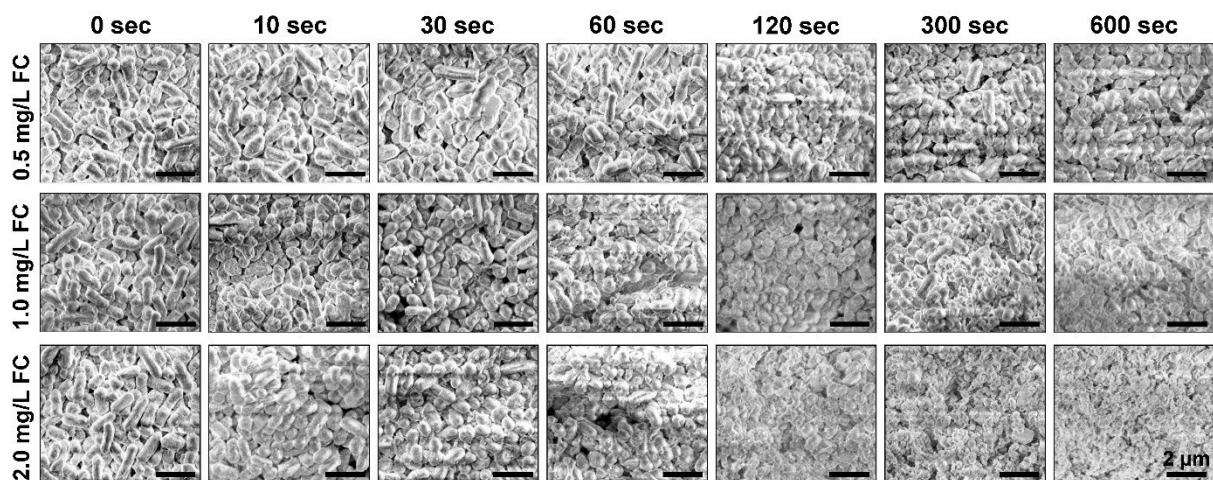

Fig. 3 Representative SEM images of *S. enterica* treated with various initial FC doses. Images corresponding to 0 sec refer to the control sample, *i.e.*, prior to chlorine addition.

3.3 Live/Dead assay for cell survival

Representative immunofluorescence images of *E. coli* exposed to three different levels of initial FC were shown in **Fig. 4**. Representative images for *E. coli* suspensions with known live/dead cell ratios were also shown (Fig 4A). When the suspension consisted of 100% live cells

(100/0 in Fig. 4A) only green fluorescence was observed, while only red fluorescence was evident in suspensions containing 100% dead cells (0/100 in Fig. 4A) that were obtained after 15 min of exposure to 0.25 mg·L^{-1} FC. The fluorescence images of the culture samples before chlorination (labeled *0 sec*) revealed mostly green fluorescence, which demonstrated that almost all *E. coli* were alive. Comparison between the three levels of FC indicated that the shift from green to red was faster with increasing chlorine concentration. For example, green-stained cells were visible for up to 2 min at 0.12 mg·L^{-1} FC, while they were hardly visible after 1 min exposure at 0.25 mg·L^{-1} FC. At the 0.5 mg·L^{-1} FC level, green-stained cells were almost non-existent after the first 10 sec of exposure. Similar patterns were noted from the fluorescence images of *S. enterica* exposed to the three different concentrations of FC (**Fig. 5**). At 0.5 mg·L^{-1} FC, some cells were still alive even after 600 sec of exposure, while no live cells were visible after 120 sec and 60 sec at 1 and 2 mg·L^{-1} FC respectively.

In line with the SEM image analysis, the qualitative fluorescence images agree with the quantitative cell survival data (Fig. 1). Since the red dye can only penetrate damaged cells, these results could be interpreted in terms of the cell membrane damage. For instance, SEM images for initial FC levels of 0.5 mg·L^{-1} after 10 sec of chlorination revealed damages to the cellular surface while the fluorescence staining shows that most of the cells were dead after 10 sec. Thus, the combination of fluorescence labeling and SEM images reveal corroborative and complementary information about the inactivation process of *E. coli* and *S. enterica* by free chlorine. It appears that the major mechanism of disinfection is through the destruction of cellular membrane organization and possibly membrane proteins, causing deformation in cell structure and functionality.[18, 26]
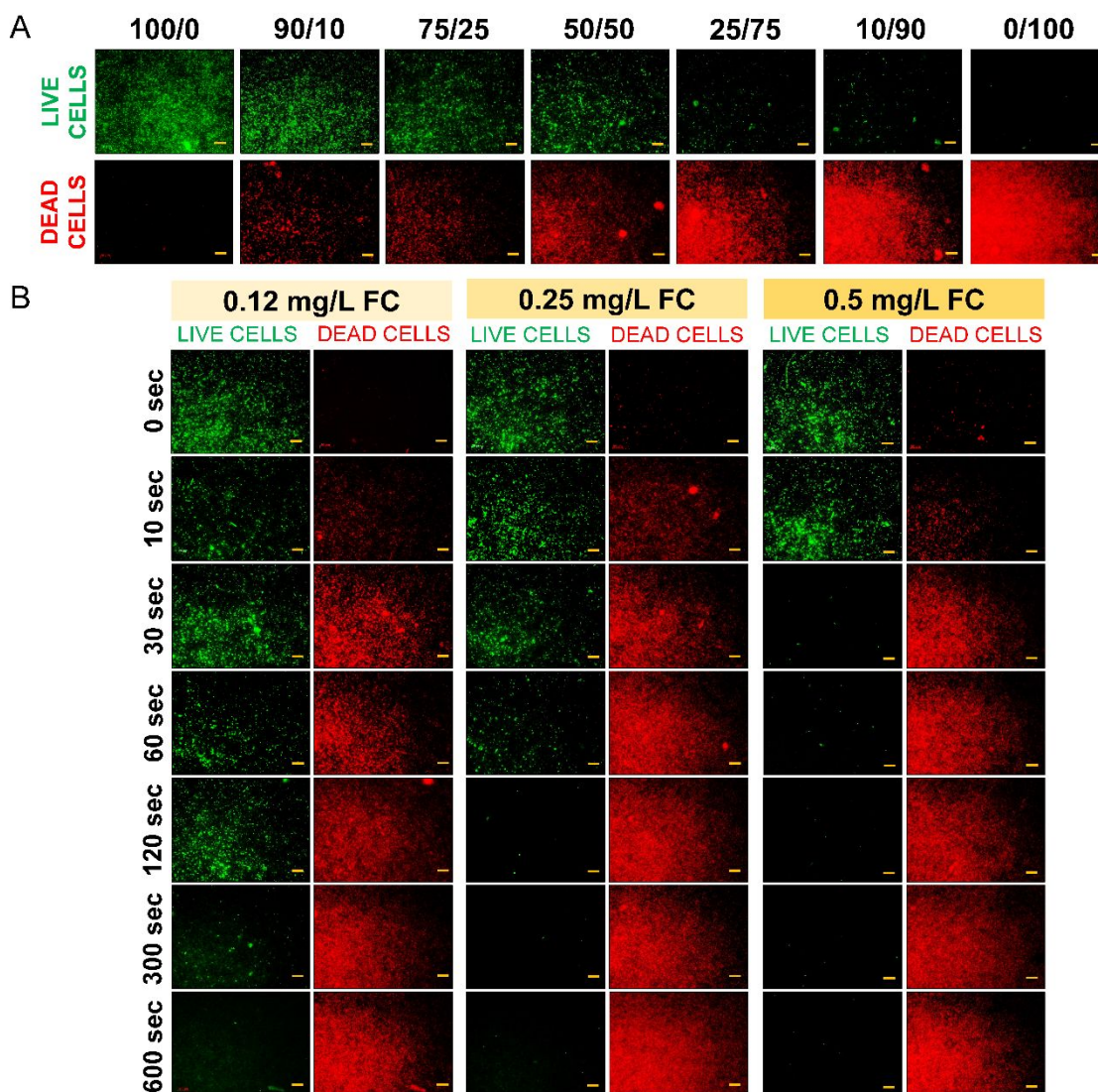
Fig. 4 Fluorescence microscopy detection of *E. coli* during chlorination. (A) Representative images for suspensions with known live/dead proportions. (B) Representative images for treated solutions under different concentration of free chlorine. Reaction conditions: pH = 7.1, T = 4 °C, initial concentration of bacteria: ~ 10^6 MPN·mL^{-1}. Scale bar: 20 µm.
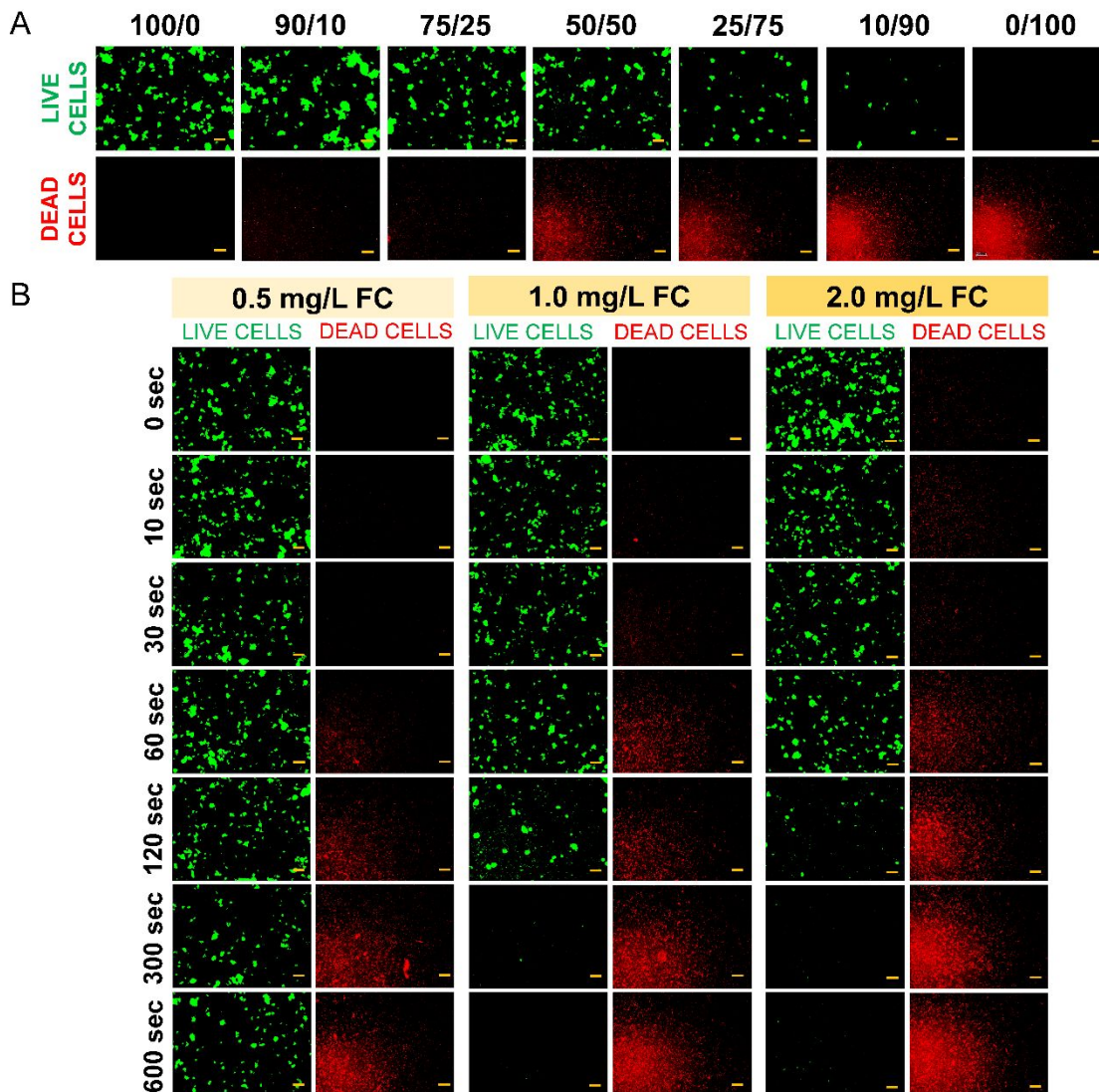
Fig. 5 Fluorescence microscopy detection of *S. enterica* during chlorination. (A) Representative images for suspensions with known live/dead proportions. (B) Representative images for treated solutions under different concentration of free chlorine. Reaction conditions: pH = 7.1, T = 4 °C, initial concentration of bacteria: ~ 10^6 MPN·mL^{-1}. Scale bar: 20 μm.

### 3.4 Live/Dead cell count from fluorescence microplate reader

Conventionally, the cell counts for bacteria inactivation by chlorination are represented in terms of the culture based MPN method to enumerate the number of live cells. Despite its

simplicity, such culture-based methods have certain disadvantages, including longer duration to measure outcomes, inaccuracies in quantification, higher probability of false-positives, and the possibility that some cells could become VBNC during disinfection.[40, 41] In this study, we quantified the number of viable cells using a fluorescence spectroscopy-based live/dead assay. After generating the standard curve (**Suppl. Fig. 1**) for suspensions with a known *E. coli* live/dead ratio ($Ratio_{G/R}$), the viable cell percentage was obtained for disinfection samples (**Fig. 6**). Results from the MPN method (Fig. 1) and fluorescence spectroscopy (Fig. 6) have strikingly similar trends. Further analysis revealed that, on average, the percentage of viable cells noted from spectroscopy method was higher by (3.45% ± 1.9%) for *E. coli* and by (3.49% ± 2.3%) for *S. enterica,* than the MPN method ($p < 0.01$ in both the cases). This suggests that chlorination might induce a loss of culturability although the bacteria are still viable,[17, 36] and that rapid, direct measurement using a fluorescence spectroscopy appears to capture cell survival data with higher fidelity and accuracy than the MPN method.
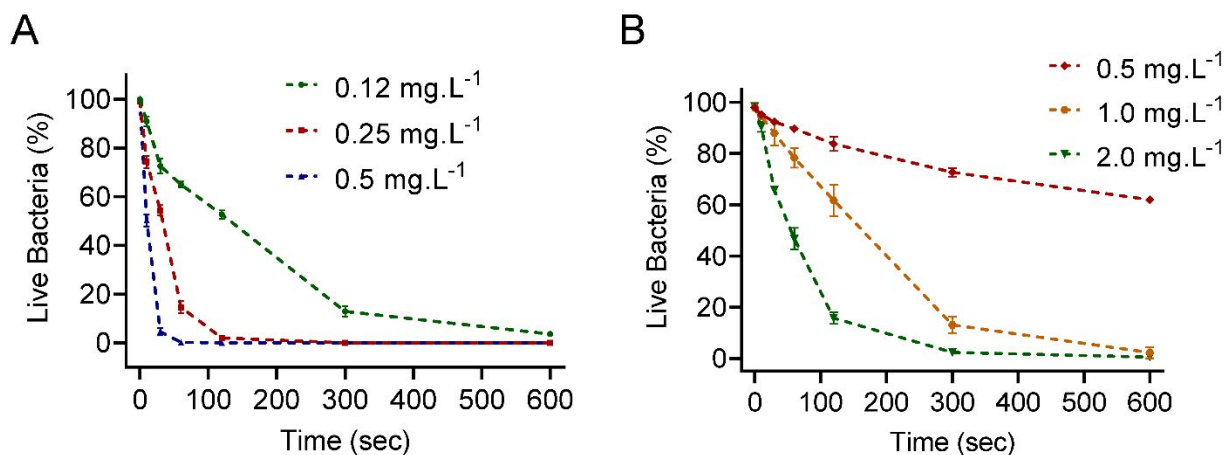
Fig. 6 *E. coli* (**A**) and *S. enterica* (**B**) suspensions were each treated with three different free chlorine concentrations, and their viability quantified using Live/Dead fluorescence spectroscopy (i.e., fluorescence microplate reader). Reaction conditions: pH = 7.1, T = 4 °C, initial concentration of bacteria: ~ 10^6 MPN·mL^{-1}.

3.5 Chlorination effect on bacteria metabolism and culturability

To assess the chlorine impact on bacteria metabolism and thus their proliferation, a MTT colorimetric assay was performed. The OD_{540} absorbance values obtained for *E. coli* activity after chlorine treatment at three different concentrations are shown in **Fig. 7A**. The OD_{540} values and growth inhibition were in line with the MPN method and fluorescence spectroscopy results detailed above. The OD_{540} values decreased with time for all concentrations, and with increasing FC concentration at each time point. The OD_{540} data fitted well to a one-phase exponential decay model $[y = y_0 + a * e^{-b * x}]$ at each chlorine concentration tested ($R^2 > 0.97$, $p < 0.005$ in all the cases), with the values of y_0, a and b in the range $0.042 - 0.15$, $0.357 - 0.55$, and $0.017 - 0.086$, respectively. By extension, cell growth was inhibited over the 10 min period at all initial FC concentrations as well as with increasing concentration at each time point. The inhibition data fitted well to an exponential plateau model $[y = y_m * (1 - e^{-k * x})]$ at each chlorine concentration tested ($R^2 > 0.96$, $p < 0.001$ in all the cases), with the values of y_m and k in the range $0.718 - 0.928$ and $0.0168 - 0.08$, respectively.

The OD_{540} absorbance values for *S. enterica* activity after chlorine treatment at various initial FC were shown in **Fig. 7B**. The OD_{540} values and growth inhibition agree with the MPN method and fluorescence spectroscopy results detailed above. The OD_{540} values decreased with time for all concentrations, and with increasing FC concentration at each time point. The OD_{540} data fitted well to a one-phase exponential decay model $[y = y_0 + a * e^{-b * x}]$ at each chlorine concentration tested ($R^2 > 0.95$, $p < 0.0024$ in all the cases), with the values of y_0, a and b in the range of $0.186 - 0.305$, $0.422 - 0.613$, and $0.0204 - 0.0863$, respectively. *S. enterica* growth decreased significantly over time at all initial FC concentrations and with increasing concentration at each time point. The inhibition data fitted well to an exponential plateau model $[y = y_m * (1 - e^{-k * x})]$

at each chlorine concentration tested ($R^2 > 0.95$, $p < 0.003$ in all the cases), with the values of y_m

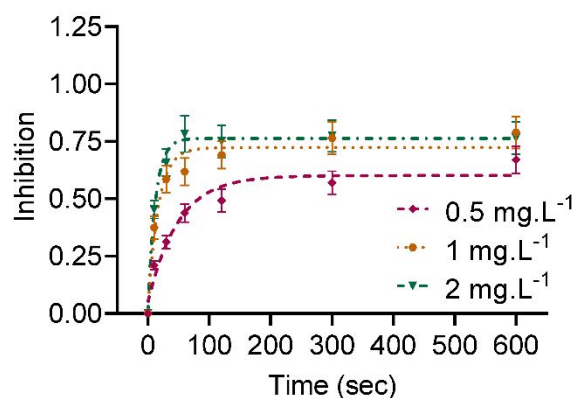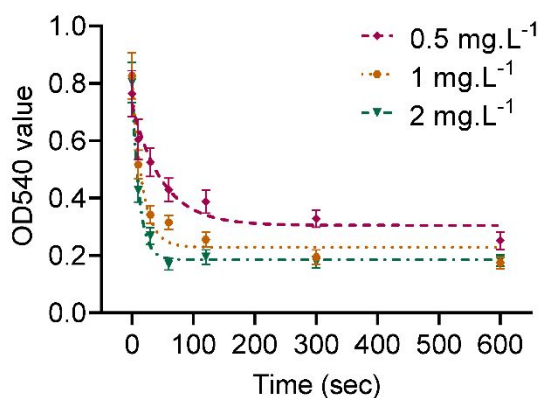and k in the range $0.6012 - 0.763$ and $0.0204 - 0.0826$, respectively.
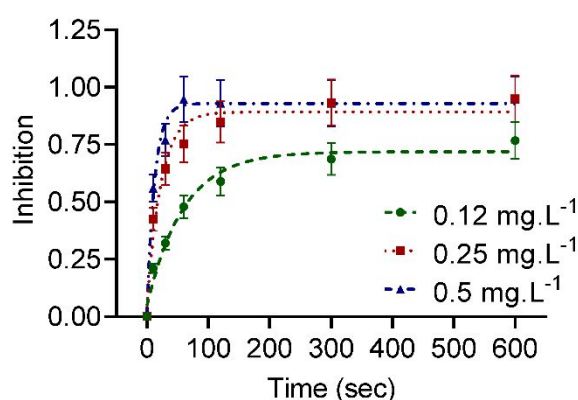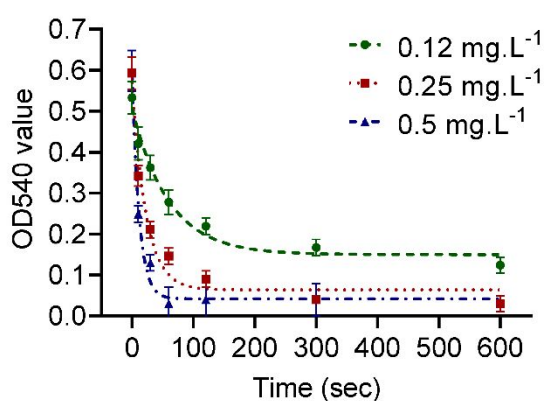
Fig. 7 The inhibition of cell growth caused by free chlorine was quantified via the MTT assay. The OD absorbance values and cell proliferation inhibition (%) after treatment with chlorine was quantified for *E. coli* (**A**) and *S. enterica* (**B**). Reaction conditions: pH = 7.1, T = 4 °C, initial concentration of bacteria: ~ 10^6 MPN·mL⁻¹. The OD_{540} data was fitted to a one-phase exponential decay model of the form $[y = y_0 + a * e^{-b * x}]$, while the inhibition data was fitted well to an exponential plateau model of the form $[y = y_m * (1 - e^{-k * x})]$ at each chlorine concentration tested, and the model parameters were obtained for comparison across the cases. The symbols indicate the average ± SD of the data, while the dotted lines indicate the respective model fits for data sets.

21

The growth inhibition of *E. coli* after 30 sec was around 32%, 64%, and 74% respectively, after exposure to 0.12, 0.25 and 0.5 mg·L⁻¹ FC. Similarly, the growth inhibition of *S. enterica* after a 30-sec exposure to 0.5, 1, and 2 mg·L⁻¹ FC was around 31%, 58%, and 66%, respectively. These results suggest that cells can remain VBNC or *persisters* during the disinfection process, escape detection by conventional counting assays, continue to passively consume nutrients, participate in the transcription process, and could return to lethal active state after reduction in external stress levels. [42-44]

3.6 Chlorine effects on total and intracellular ATP

Since ATP is the chemical energy that cells use for their metabolic activities, its levels could be an indicator of microbial activity and viability. The changes in total and intracellular ATP levels during the disinfection treatment of *E. coli* (**Fig. 8**) were obtained using an ATP determination kit based on the standard curve for known ATP levels (**Suppl. Fig. 2**). During chlorination, ATP was released from the cells due to the damaged membrane, with the amount of ATP released depending on the initial FC levels. The total and intracellular ATP remained unchanged for the untreated control cell suspension over the 10 min duration of the experiment, for both *E. coli* and *S. enterica*.

Before starting the disinfection experiments the *E. coli* concentration was around 6-log MPN·mL⁻¹ (**Fig. 8a**) with 91.8% ± 1.4% intracellular (7.35 ± 0.17 nM) and 8.2% ± 1.4% extracellular ATP (0.66 ± 0.11 nM). Exposure to chlorine increased the total ATP in a FC concentration dependent manner, possibly due to the damaged metabolic pathways and the imbalance in the normal equilibrium between synthesis and utilization of generated ATP.[45] However, the increase in total ATP was brief (up to a minute) post-chlorination, beyond which the total ATP levels remained constant. The intracellular ATP content significantly decreased during

22

the disinfection process with increasing FC levels and exposure time, most likely via ATP leakage from the cells due to damaged cellular membrane. Thus, the loss in intracellular ATP could also be an indicator of cellular membrane damage. Similar patterns were evident in total and intracellular ATP levels in *S. enterica* cultures exposed to FC (**Fig. 8b**), although the total ATP levels in *S. enterica* were generally significantly higher than that in *E. coli*.
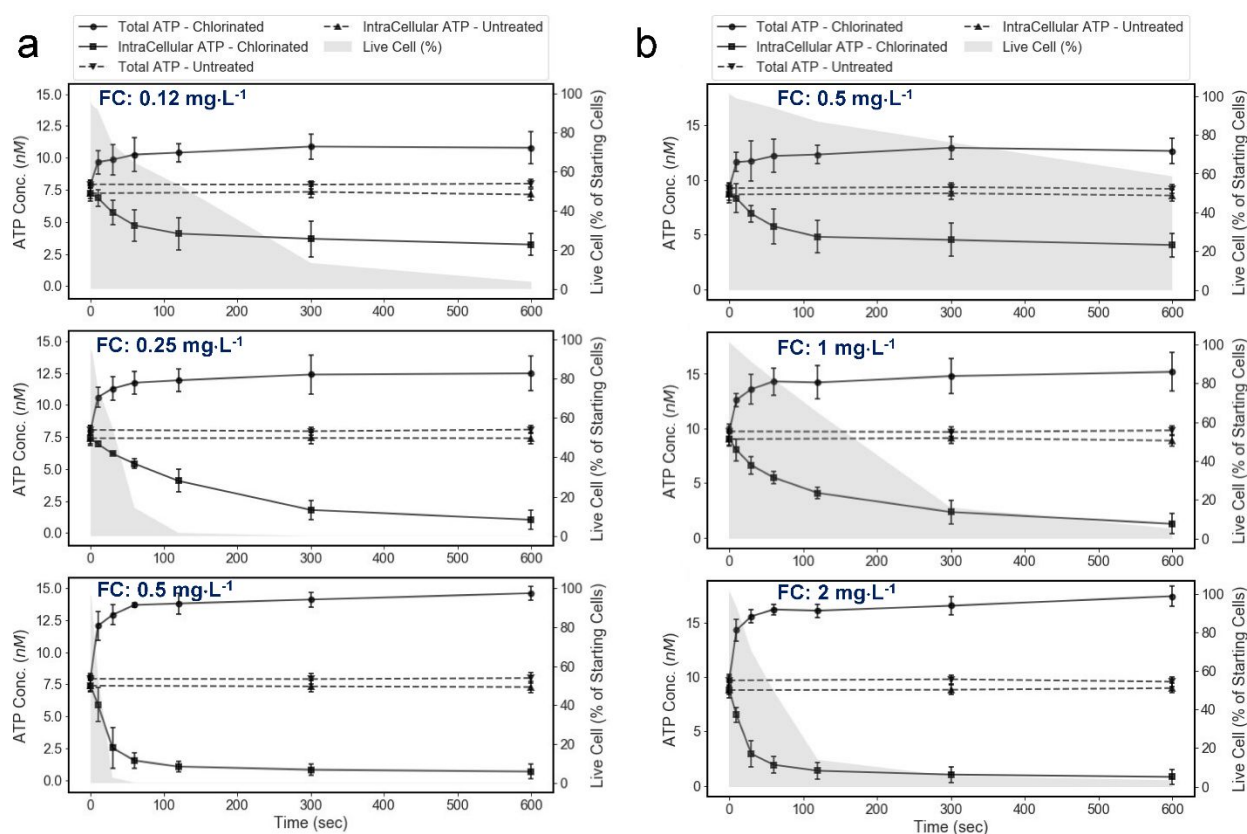
Fig. 8 Effects of initial free chlorine levels on ATP levels in *E. coli* (**a**) and *S. enterica* (**b**) cultures. *E. coli* was exposed to 0.12, 0.25 and 0.5 mg·L^{-1} FC levels, while *S. enterica* was exposed to 0.5, 1.0 and 2.0 mg·L^{-1} FC. The grey shaded area in each plot shows the percentage of live bacteria (N = N$_0$) from the fluorescence spectroscopy data. A strong correlation between intracellular ATP levels and bacteria survival at that time point is evident.

Low doses of chlorine (< 5 mg·L^{-1}) reportedly affect membrane permeability and consequently increase extracellular ATP levels, indicating ATP leakage. [16] External stresses such as pH and

osmotic pressure were shown to increase ATP levels in *E. coli*, partly via upregulation in transcription of genes coding for glycolytic enzymes and glucose metabolism pathways, which help these cells survive and thrive in harsh environments (e.g., human gut). [46] The small size and neutral charge of hypochlorous acid enables passive diffusion through the membrane of gram negative cells (*E. coli*, *Salmonella*), impair membrane proteins involved in energy synthesis and transport, leading to ATP hydrolysis. [42, 47] Gram-negative bacteria such as *E. coli* mitigate chlorine-induced oxidative stress and protect bacterial proteome by altering their metabolism pathways related to amino acid metabolism, and lipid and nucleotides synthesis, [48] and release of heat-shock proteins. [49] The expression of metabolites such as arginine and betaine increased in non-pathogenic O157:H7 strain of *E. coli* exposed to 4 mg·L^{-1} of FC for ten minutes, whereas levels of a few amino acids (Asp, Ile, Met, Tyr), organic acids (acetic acid, α-ketoglutaric acid, fumaric acid, γ-aminobutyric acid), nucleotide-related compounds (ATP, NAD, ADP), and others (1,2-propanediol, Phosphorylcholine, Putrescine) decreased, compared to cells treated with distilled water. [50] Whether such trends in metabolites hold in cultures exposed to residual FC levels (≤ 2 mg·L^{-1}) remain to be investigated.

3.7 Flow Cytometry analysis of changes in membrane potential

Flow Cytometry analysis was done to quantitively assess the changes in membrane potential of the chlorinated cells and assess disinfection efficiency. [51] This was achieved using staining with DiOC2(3) and generating scatter plots of green versus red fluorescence. CCCP was used to generate depolarized control cell populations, and reasonable gates were drawn around the depolarized control group. The population-level changes in cellular membrane potential during the chlorination process of *E. coli* and *S. enterica* were expressed in **Fig. 9**. Representative flow

24

cytometry plots at various FC levels from *E. coli* analysis were shown in **Fig. 9A**. The plots for untreated samples (presented as "0 sec") indicate that untreated viable cells are completely out of the fixed depolarized gate with a shift toward red fluorescence. This is because DiOC2(3) stains all bacterial cells green fluorescence, but the fluorescence shifts toward red emission as the dye molecules self-associate at the higher cytosolic concentrations caused by larger membrane potentials.[26] With increasing contact time in chlorine disinfection, the red fluorescence gradually diminished, exhibiting a shift of the clusters towards the fixed depolarized gate, resulting in complete migration to the depolarized zone. This indicates that the cell membrane potential of *E. coli* is declining during the chlorine disinfection process, mostly due to effects on structural membrane integrity. Similar trends were noted for *S. enterica* as well (flow cytometry plots not shown here).

The percentage of depolarized cells was quantified from these images using FlowJ software (https://www.flowjo.com/) and shown in **Fig. 9, B-C**. The rate of membrane potential loss or depolarization was faster at the higher FC levels. This is because the cellular membrane damage increased with increasing FC concentration, as noted in previous sections. The depolarized *E. coli* density reached a plateau after the first 2 min at FC $\geq$ 0.5 mg·L^{-1} and after 5 min at 0.12 mg·L^{-1} FC. However, the depolarized *S. enterica* density took 5 min to reach a plateau even at FC $\geq$ 1 mg·L^{-1}, indicating their ability to withstand chlorine. Others also have reported that chlorine treatment led to a reduction in cellular membrane potential,[17] and with prolonged exposure caused both a reduction in the intact cell count and fluorescence intensity, indicating a breakdown of the cell membrane. ATP release from FC-induced damage in gram-negative bacteria correlated with membrane damage detected with flow cytometry in our study. Interestingly, such extracellular ATP released by *E. coli* upon exposure to high FC doses (> 5 mg·L^{-1}) contributed to bacteria

regrowth potentially offsetting the efficacy of sanitizers at high doses, [47] although we haven't noted

such bacterial regrowth in our study at residual FC doses.
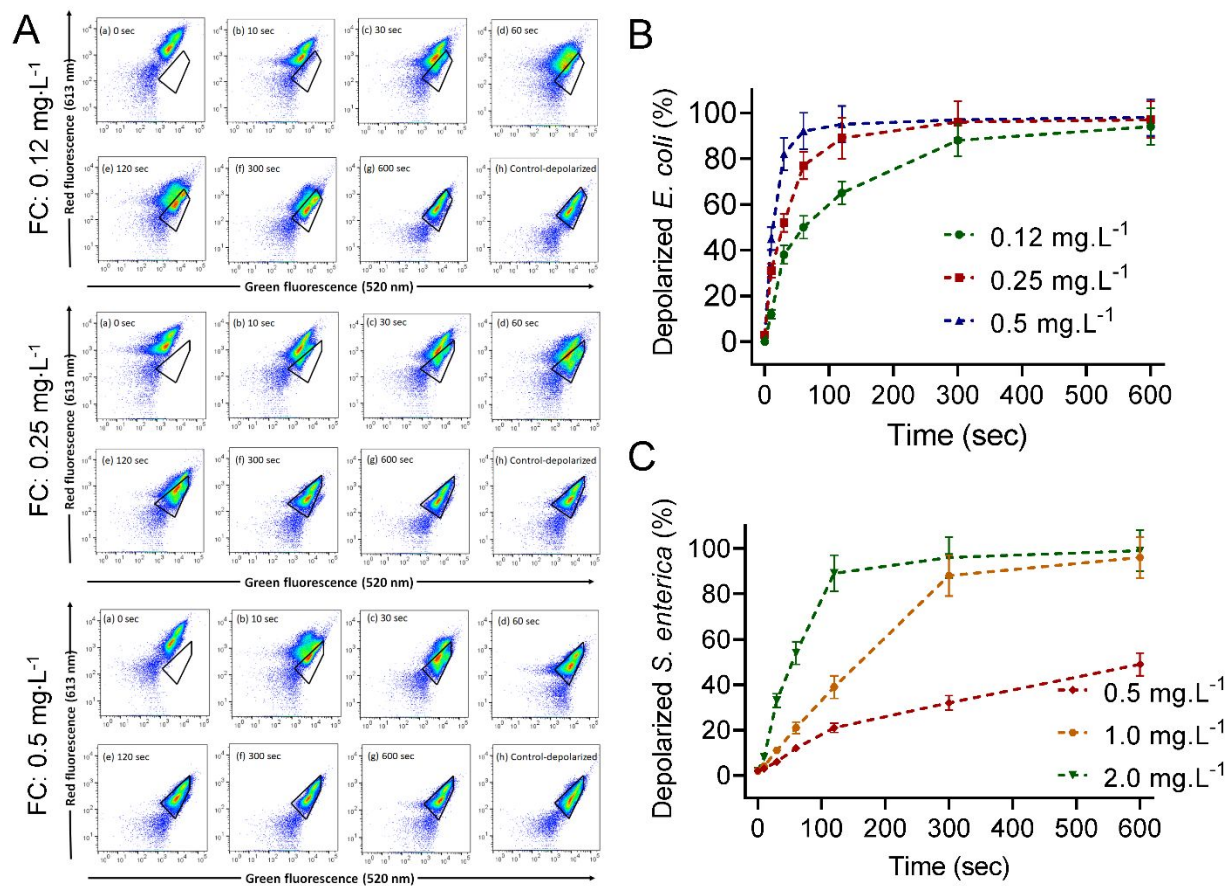
Fig. 9 (A) Flow cytometry analysis and membrane potential results for *E. coli* after exposure to 0.12, 0.25, and 0.5 mg·L^{-1}. At each concentration of FC, analysis was done at 0, 10, 30, 60, 120, 300, and 600 sec time points, with appropriate controls. Similar analysis was done for *S. enterica* cultures as well. Depolarization of *E. coli* (**B**) and *S. enterica* (**C**) under exposure to three FC levels.

The loss of membrane integrity could be a gradual and time-delayed process which would be

well captured quantitatively by a sensitive assay such as flow cytometry. Conventional plate

counting assays, on the other hand, will not account for compromises in cell membrane if the cell

embeds as part of a colony. Our results suggest that with increasing FC concentration and/or

exposure time, the culturability of *E. coli* and *S. enterica* decreased coinciding with depolarization

of more cells (Figs. 1 and 9). However, the depolarization was more gradual whereas the drop in

cell survival was more dramatic, making the former a conservative indicator of the latter. This

hints at stochasticity in the disinfection process, even within such short exposure, as well as

heterogeneity in cells with varying susceptibility to FC assault. Based on our findings, the broad

mechanisms by which various doses of residual FC differentially affects *E. coli* and *S. enterica*

were depicted in **Fig. 10**. The list is not comprehensive as there could be other signaling pathways

that are impacted at these culture conditions.

E. coli				*S. enterica*		
Low FC (0.12 mg·L⁻¹)	**Medium FC** (0.25 mg·L⁻¹)	**High FC** (0.5 mg·L⁻¹)		**Low FC** (0.5 mg·L⁻¹)	**Medium FC** (1.0 mg·L⁻¹)	**High FC** (2.0 mg·L⁻¹)
Slow inactivation	*Fast inactivation*	*Rapid cell death*		*Less inactivation*	*Delayed inactivation*	*Slow inactivation*
Slight membrane damage	*Moderate membrane damage*	*Severe membrane damage*		*Intact membrane*	*Minor membrane damage*	*Major membrane damage*
Wrinkled surface	*Hole formation & shrinkage*	*Structure collapse*		*Cell rounding*	*Clustering, fusion & shrinkage*	*Structural damage*
Slow decay in metabolism	*Rapid decay in Metabolism*	*Rapid decay in metabolism*		*Delayed decay in metabolism*	*Slow decay in cell metabolism*	*Slow decay in cell metabolism*
Slight increase in Total ATP	*Significant increase in Total ATP*	*Rapid increase in Total ATP*		*Slight increase in Total ATP*	*Delayed increase in Total ATP*	*Rapid increase in Total ATP*
Slight decrease in intracellular ATP	*Delayed decrease in intracellular ATP*	*Rapid decrease in intracellular ATP*		*Slight decrease in intracellular ATP*	*Delayed decrease in intracellular ATP*	*Rapid decrease in intracellular ATP*
Moderate cell depolarization	*Significant cell depolarization*	*Rapid cell depolarization*		*Slower cell depolarization*	*Delayed cell depolarization*	*Rapid cell depolarization*
Delayed cell death	*Rapid cell death*	*Rapid cell death*		*Minimal cell death*	*Delayed cell death*	*Moderate cell death*

Fig. 10 Schematic illustrating the various mechanisms by which residual FC affects the survival, morphology, cell membranes, cellular organelles and function, and metabolism and ATP levels in gram-negative bacteria cultures. The list may not be comprehensive, and the DNA damage and protein aggregation mechanisms were based on pertinent literature. [42]

4 Conclusions

In many areas along the food chain (e.g., pre- and post-harvest, chlorine is widely used. Despite significant progress having been made in combating foodborne illnesses caused by bacteria, viruses and parasites, millions of Americans continue to be affected and thousands die annually. There is a critical need to (i) identify the minimum chlorine levels (free chlorine, not the total chlorine) needed to maximize the impact on sanitation without excessive chlorination, (ii) elucidate the fundamental mechanisms by which chlorine deactivates and destroys pathogens common to food industry, (iii) integrate mathematical modeling and statistical analysis for informed risk analysis and management of microbial threats, (iv) implement real-time modulators of free chlorine levels to meet pathogen ebb and surge, and (v) develop high-throughput and high-fidelity protocols for the rapid diagnosis of free chlorine effects on various pathogen types. Studies such as ours will help identify the minimum free chlorine levels and exposure duration critically required for complete inactivation of the most common bacterial types and determine the mechanism(s) by which such inactivation occurs at the sub-cellular level. Similar approaches could be extended for investigating the interplay between other sanitizers and bacteria (e.g., *Campylobacter*, *Vibrio*) combinations.

Residual free chlorine level and its contact time are used as reliable proxy indicators for disinfection efficacy and chemical safety in a variety of applications including drinking and swimming water treatment and distribution systems. Thus, elucidating the mechanisms by which such inactivation would occur is very important. While chlorination effects on bacteria in the absence of organic matter was studied here, similar trends could be expected even in its presence, especially at such low chlorine concentrations,[18] which forms part of our future studies. Results from such studies could also help in fine-tuning FC dosing strategies for fresh produce wash

process or meat processing plants where excess FC levels could lead to the formation of undesirable reaction by-products.

Conflicts of interest

There are no conflicts to declare.

References

1.   Y. Li, M. Yang, X. Zhang, J. Jiang, J. Liu, C. F. Yau, N. J. D. Graham and X. Li, *Water Res*, 2017, **108**, 339-347.
2.   C. Qiu, W. He, Y. Li, F. Jiang, Y. Pan, M. Zhang, D. Lin, K. Zhang, Y. Yang, W. Wang and P. Hua, *Chemosphere*, 2022, **305**, 135417.
3.   F. Lopez-Galvez, A. Allende and M. I. Gil, *Curr Opin Food Sci*, 2021, **38**, 46-51.
4.   C. Shen, Y. Luo, X. Nou, Q. Wang and P. Millner, *J Food Prot*, 2013, **76**, 386-393.
5.   T. J. Fu, Y. Li, D. Awad, T. Y. Zhou and L. Liu, *Food Control*, 2018, **94**, 212-221.
6.   V. M. Gomez-Lopez, A. S. Lannoo, M. I. Gil and A. Allende, *Food Control*, 2014, **42**, 132-138.
7.   Y. Luo, X. Nou, Y. Yang, I. Alegre, E. Turner, H. Feng, M. Abadias and W. Conway, *J Food Prot*, 2011, **74**, 352-358.

8.   S. Van Haute, I. Tryland, C. Escudero, M. Vanneste and I. Sampers, *LWT*, 2017, **75**, 301-304.
9.   S. Chowdhury, M. J. Rodriguez and R. Sadiq, *J Hazard Mater*, 2011, **187**, 574-584.
10.   S. Van Haute, I. Sampers, K. Holvoet and M. Uyttendaele, *Appl Environ Microbiol*, 2013, **79**, 2850–2861.
11.   M. I. Gil, F. Lopez-Galvez, S. Andujar, M. Moreno and A. Allende, *Food Control*, 2019, **100**, 46-52.
12.   R. S. Breed and W. D. Dotterrer, *J Bacteriol*, 1916, **1**, 321–331.
13.   W. G. Cochran, *Biometrics*, 1950, **6**, 105-116.
14.   S. Chen, X. Li, Y. Wang, J. Zeng, C. Ye, X. Li, L. Guo, S. Zhang and X. Yu, *Water Res*, 2018, **142**, 279-288.
15.   D. B. Roszak and R. R. Colwell, *Microbiol Rev*, 1987, **51**, 365-379.
16.   L. Xu, C. Zhang, P. Xu and X. C. Wang, *J Environ Sci (China)*, 2018, **65**, 356-366.
17.   R. Cheswick, G. Moore, A. Nocker, F. Hassard, B. Jefferson and P. Jarvis, *Environ Technol Innov*, 2020, **19**, 101032.
18.   R. Virto, P. Manas, I. Alvarez, S. Condon and J. Raso, *Appl Environ Microbiol*, 2005, **71**, 5022-5028.
19.   Y. W. Lin, D. Li, A. Z. Gu, S. Y. Zeng and M. He, *Chemosphere*, 2016, **144**, 2165-2174.
20.   Z. G. Erosy, O. Dinc, B. Cinar, S. T. Gedik and A. Dimoglo, *LWT*, 2019, **102**, 205-213.
21.   R. Cheswick, E. Cartmell, S. Lee, A. Upton, P. Weir, G. Moore, A. Nocker, B. Jefferson and P. Jarvis, *Environ Int*, 2019, **130**, 104893.
22.   Y. Lee, S. Imminger, N. Czekalski, U. von Gunten and F. Hammes, *Water Res*, 2016, **101**, 617-627.
23.   D. E. Turner, E. K. Daugherity, C. Altier and K. J. Maurer, *J Am Assoc Lab Anim Sci*, 2010, **49**, 190-195.
24.   G. Wen, X. Xu, T. Huang, H. Zhu and J. Ma, *Water Res*, 2017, **125**, 132-140.
25.   I. Ofori, S. Maddila, J. Lin and S. B. Jonnalagadda, *J Water Process Eng*, 2018, **26**, 46-54.
26.   D. Kennedy, U. P. Cronin and M. G. Wilkinson, *Appl Environ Microbiol*, 2011, **77**, 4657–4668.
27.   Z. Ye, S. Wang, T. Chen, W. Gao, S. Zhu, J. He and Z. Han, *Sci Rep*, 2017, **7**, 6279.
28.   Y. Luo, B. Zhou, S. Van Haute, X. Nou, B. Zhang, Z. Teng, E. R. Turner, Q. Wang and P. D. Millner, *Food Microbiol*, 2018, **70**, 120-128.
29.   G. C. White, in *The Handbook of Chlorination*, Nostrand Reinhold, New York, 2nd edn., 1986, ch. 6, pp. 256-393.
30.   C. Tong, H. Hu, G. Chen, Z. Li, A. Li and J. Zhang, *Environ Res*, 2021, **195**, 110897.
31.   E. Cabrera-Diaz, T. M. Moseley, L. M. Lucia, J. S. Dickson, A. Castillo and G. R. Acuff, *J Food Prot*, 2009, **72**, 295-303.
32.   S. E. Niebuhr, A. Laury, G. R. Acuff and J. S. Dickson, *J Food Prot*, 2008, **71**, 714-718.
33.   M. Abnavi, C. R. Kothapalli, D. Munther and P. Srinivasan, *Int J Food Microbiol*, 2021, **356**, 109364.
34.   M. Deborde and U. von Gunten, *Water Res*, 2008, **42**, 13-51.
35.   B. Zhou, Y. Luo, X. Nou, S. Lyu and Q. Wang, *Food Microbiol*, 2015, **50**, 88-96.
36.   C. J. Higmore, J. C. Warner, S. D. Rothwell, S. A. Wilks and C. W. Keevil, *MBio*, 2018, **9**, e00540-00518.
37.   D. I. Pattison and M. J. Davies, *Chem Res Toxicol*, 2001, **14**, 1453–1464.
38.   T. Obe, R. Nannapaneni, C. S. Sharma and A. Kiess, *Poult Sci*, 2018, **97**, 951–961.

39.   R. Capita, F. Riesco-Peláez, A. Alonso-Hernando and C. Alonso-Calleja, *Appl Environ Microbiol*, 2014, **80**, 1268–1280.
40.   S. Sutton, *J Valid Technol*, 2010, **16**, 35-38.
41.   L. Kuai, A. A. Nair and M. F. Polz, *Appl Environ Microbiol*, 2001, **67**, 3168-3173.
42.   W. S. da Cruz Nizer, V. Inkovskiy and J. Overhage, *Microorganisms*, 2020, **8**, 1220.
43.   L. Li, N. Mendis, H. Trigui, J. D. Oliver and S. P. Faucher, *Front Microbiol*, 2014, **5**, 258.
44.   X. Zhao, J. Zhong, C. Wei, C. W. Lin and T. Ding, *Front Microbiol*, 2017, **8**, 1-16.
45.   J. Wang, M. Sui, B. Yuan, H. Li and H. Lu, *Sci Total Environ*, 2019, **648**, 271-284.
46.   W. Zhang, X. Chen, W. Sun, T. Nie, N. Quanquin and Y. Sun, *Genes (Basel)*, 2020, **11**, 991.
47.   A. Nescerecka, T. Juhna and H. , F., *Water Res*, 2016, **101**, 490-497.
48.   Q. Liu, L. Chen, A. K. C. Laserna, Y. He, X. Feng and H. Yang, *Food Control*, 2020, **110**, 107026.
49.   C. V. Goemans and J. F. Collet, *F1000Research*, 2019, **8**, 1678–1684.
50.   Y. Wang, J. Wu and H. Yang, *Food Control*, 2022, **131**, 108458.
51.   A. Nocker, R. Cheswick, P.-M. de la Rochere, D., M. Denis, T. Leziart and P. Jarvis, *Environ Technol*, 2017, **38**, 891-900.